IEEE Access
Multidisciplinary | Rapid Review | Open Access Journal

Received January 21, 2022, accepted March 3, 2022, date of publication March 14, 2022, date of current version March 23, 2022.

Digital Object Identifier 10.1109/ACCESS.2022.3159337

Planar FSS Based Dual-Band Wire Monopole Antenna for Multi-Directional Radiation With Diverse Beamwidths

AYAN CHATTERJEE[1], (Member, IEEE), SOUMEN BANERJEE[1], (Senior Member, IEEE), JAROSLAV FRNDA[2,3], (Senior Member, IEEE), AND MAREK DVORSKY[3]

[1]Department of Electronics and Communication Engineering, University of Engineering and Management, Kolkata, West Bengal 700160, India
[2]Department of Quantitative Methods and Economic Informatics, University of Zilina, 010 26 Zilina, Slovakia
[3]Department of Telecommunications, VSB—Technical University of Ostrava, 70800 Ostrava, Czech Republic

Corresponding author: Soumen Banerjee (prof.sbanerjee@gmail.com)

This work was financially supported by the VSB—Technical University of Ostrava, the Ministry of Education, Youth and Sports, Czech Republic, under Grant SP2022/5 and Grant SP2022/18.

ABSTRACT In this paper, two planar Frequency Selective Surfaces (FSS) with dissimilar configurations along with monopole antenna exhibiting dual-band response at 3 GHz and 5.5 GHz is presented. One of the surfaces with two reflectors is reflective at 5.5 GHz and transmissive at 3 GHz, whereas the response is opposite for the FSS in another flat reflector. Accordingly the antenna exhibits directive radiation at both the frequencies, however in two opposite directions. Unit cell of the FSS at 3 GHz is on the order of $\lambda_g/11$, leading to low-profile design. With different orientations of the reflectors, beamwidths at 3 GHz and 5.5 GHz are different leading to different peak gains of 7.1 dBi and 12.2 dBi respectively. The composite antenna-FSS with a dimension on the order of $1.1\lambda \times 1.1\lambda \times 0.2\lambda$ exhibits diverse beam radiation. The radiation at 3 GHz can be used in applications involving wide coverage area, whereas at 5.5 GHz the antenna can be used in applications involving smaller beamwidths such as satellite communication, Ground Penetrating Radar etc.

INDEX TERMS Dual-band antenna, frequency selective surface, planar reflector, beam diversity.

I. INTRODUCTION

Antenna diversity can be realized in terms of polarization diversity, pattern diversity, spatial diversity and transmitter/receiver diversity. Antenna diversity in shape and beamwidth of radiation pattern are effective in reducing multi-path interference leading to reliable wireless link, exhibiting multiple modes of operation in mobile applications etc. and thus gaining significant attention [5]–[10]. Adaptive patterns of such antennas exhibit higher gain in a certain direction for enhanced signal strength [1]–[4] and radiation with wide beamwidth and adequate gain [11]–[14] in other direction leading to multi-directional radiation. Diversity in radiation can be implemented using two or more closely spaced antenna elements with different patterns. The implementation of pattern diversity often needs the use of arrays for radar applications and long distance communication. However certain applications such as indoor communication does not need much higher gain and thus the purpose can be solved with few antenna elements with various patterns. Several methods have been incorporated till date for achieving pattern diversity in antennas [15], [25]–[27]. In general, pattern diversity is achieved by co-locating more antenna elements with different radiation patterns. A dual-port diversity antenna was developed by Sifat *et al.* [4] integrating a monopole and a suspended patch exhibiting broadside radiation as well as conical radiation pattern at different frequency. Sun *et al.* proposed [15] a mono-cone antenna exhibiting pattern diversity characteristics. The ground of the microstrip antenna was used as a top loading of the mono-cone antenna leading to a large profile and complex design. The design strategy was improved with the advent of periodic structures such as electromagnetic bandgap structure (EBG), partially reflective surfaces (PRS) and frequency selective surfaces (FSS) with or without active elements in performance enhancement of various antennas [16]–[23]. So *et al.* proposed the design of a directional triple band antenna by incorporating three FSS-based screens designed to be reflective only at the desired frequency while passing the signals at other frequencies [20]. Edalati and Denidni developed an antenna offering

The associate editor coordinating the review of this manuscript and approving it for publication was Debdeep Sarkar.

omni-directional radiation with a reconfigurable beamwidth using PIN diode based PRS [22]. Krishnamoorthy *et al*. proposed the design of a pattern diversity antenna, using quarter mode substrate integrated waveguide sub-array exhibiting both broadside radiation with 7.2 dBi gain and conical radiation with 5.1 dBi gain [24].

The proposed design in the paper uses two different configurations of FSS for achieving diversity in beamwidth of the radiation from a dual band monopole antenna. The novelty of the proposed design lies in the integration of two different and simple planar and non-planar FSS reflectors with the wire monopole antenna for achieving narrow beam as well as wide beam directional radiation. Earlier monopole antenna with only a corner reflector FSS was proposed [35] to achieve directional and omni-directional radiation. However the FSS used in corner reflector affected the impedance matching as well as omni-directional radiation of the antenna in the lower frequency band which was undesired. In the proposed design, the FSS in the corner reflector is a dual layer FSS that overcome the above mentioned drawback of the design by improving impedance matching of the antenna in the lower band. Another design was proposed [36] with a curved FSS reflector in order to achieve wide coverage area by increasing antenna beamwidth. However the overall area of the structure was of the order of $2\lambda \times 2\lambda$ in comparison to the proposed design in this paper with dimension of $1.1\lambda \times 1.1\lambda$. Thus the antenna-FSS presented in this paper is more compact compared to the previous works.

In section II design of the dual-band monopole antenna is discussed followed by section III that describes the design and characteristics of the two FSS reflectors. Section III deals with the description of the antenna with the two FSS screens wherein it is discussed about how pattern diversity is achieved with high gain narrow beam radiation in one direction and moderate gain wide beam radiation in the other.

II. DUAL-BAND ANTENNA

A simple dual-band antenna with two closely-spaced rigid monopole wires is designed to achieve directional radiation by using a frequency selective corner reflector based on FSS in one band; and omni-directional radiation, in the other band. The quarter wave monopole antennas consist of metallic wires having lengths of 13.3 mm (L1) and 24 mm (L2) for achieving resonances at 5.5 GHz and 3 GHz, respectively, with an inter-element spacing of 6 mm (d1), as shown in Fig. 1 (a).

The individual antenna elements are connected by a metallic wire of length d1, which is fed for excitation. A circular ground plane is used with a diameter of 110 mm, which is close to the resonating wavelength corresponding to 3 GHz. A FR4 substrate with relative permittivity (ε_r) of 4.4 and thickness of 0.8 mm, is chosen as the substrate.

III. FSS-BASED PLANAR REFLECTORS

Two FSS reflector screens of different shapes have been considered for the present design as exhibited in Fig. 1(b).

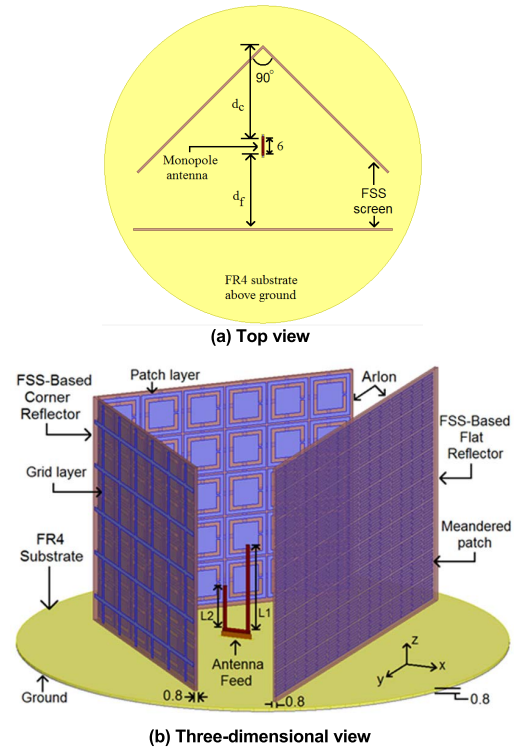

FIGURE 1. Dual-band monopole antenna with dual-layer FSS-based corner reflector (5 × 6) operating at 5.5 GHz and planar FSS (9 × 15) operating at 3 GHz.

One of the screens is designed to be reflective at 3 GHz and transmissive at 5.5 GHz, whereas the other is designed to be reflective at 5.5 GHz and transmissive at 3 GHz.

A. FREQUENCY SELECTIVE FLAT REFLECTOR

The unit cell of the frequency selective flat reflector designed to achieve bandstop response at 3 GHz is shown in Fig. 2(a) along with its dimensions. A meander line shaped patch type FSS is chosen, as because at 3 GHz, the half wavelength (50 mm) or quarter wavelength (25 mm) value is sufficiently large leading to large size of the patch if loop or cross shaped patch shape is chosen. Conventional FSS unit cells such as dipole, cross dipole, solid square patch have dimensions on the order of half-wavelength. Thus few unit cells can be accommodated in the array. In the unit cell with meander line element [27]–[30] the current path length is made larger (Fig. 2(b)) within a smaller area (6.35 mm × 6.35 mm for the proposed design) thereby reducing the unit cell dimension ($0.1\lambda_g \times 0.1\lambda_g$ where λ_g is guided wavelength) compared to the conventional unit cells at 3 GHz.

The dimensions of unit cell of the flat FSS are listed in Table 1. Arlon AD320 is chosen as the substrate having dielectric constant $\varepsilon_r = 3.2$ and loss tangent of 0.002. The dimension (6.35 mm × 6.35 mm) is of the order of $0.1\lambda_g$ with respect to guided wavelength at 3 GHz. An array of 9 × 15 elements of the FSS is designed and incorporated in the antenna above the ground plane at a spacing of d_f mm from

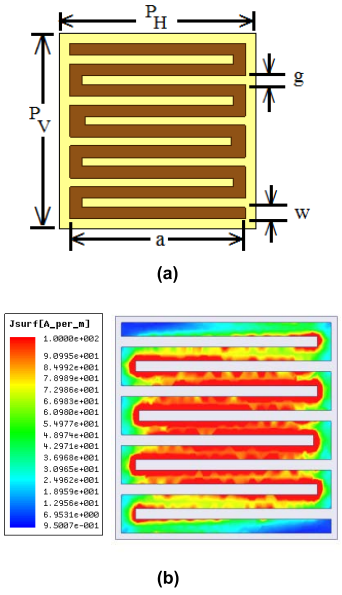

FIGURE 2. (a) Dimensions of unit cell of the flat FSS operating at 3 GHz (All dimensions in millimeters). (b) Surface current distribution (A/m) on the unit cell at 3 GHz.

TABLE 1. Dimensions of unit cell of flat FSS (3 GHz).

Parameter	$P_H = P_V$	a	w	g
Value	6.35 mm	6 mm	0.4 mm	0.3 mm

the longer monopole. The spacing is varied later in order to achieve adequate gain in both the frequency bands.

The characteristics of the flat shaped FSS are plotted in Fig. 3 and the corresponding phase responses are plotted in Fig. 4. The FSS used presents a property of transmission lower than −10 dB at 2.7-3.3 GHz frequency band with resonance at 3.01 GHz, and a bandwidth of 20%. Transmission coefficients of the FSS for different incidence angles of the plane wave (theta) in the TE plane (XZ) are also included in Fig. 3. The angular stability of the design above 45° is evident from the plot. The reflection level is close to 0 dB in the frequency band. The reflection phase variation with frequency is linear in the operating band as evident from Fig. 4 and the phase is around 180° at 3 GHz. A perfectly conducting surface also exhibits a reflection phase of 180° however over all frequencies. Thus the FSS behaves like a partially reflective surface near 3 GHz, whereas near 5.5 GHz it becomes transparent to the waves incident on it, as because the transmission is close to 0 dB at 5.5 GHz with the reflection level below −10 dB.

B. FREQUENCY SELECTIVE CORNER REFLECTOR

A frequency selective corner reflector is designed using FSS as shown in Fig. 1(b) that can reflect signals at 5.5 GHz while keeping its transmissive nature at 3 GHz. The unit cell of the FSS is shown in the Fig. 5. The top layer of the unit cell in the corner reflector is designed with the shape of a square patch loaded with split ring slot in order to incorporate the combined effect of square patch and square loop. Square patch

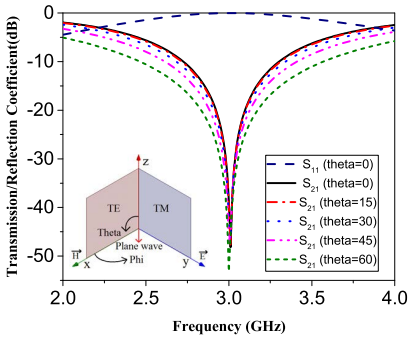

FIGURE 3. Simulated transmission coefficients of the planar FSS for normal and oblique incidence of plane wave and reflection coefficient.

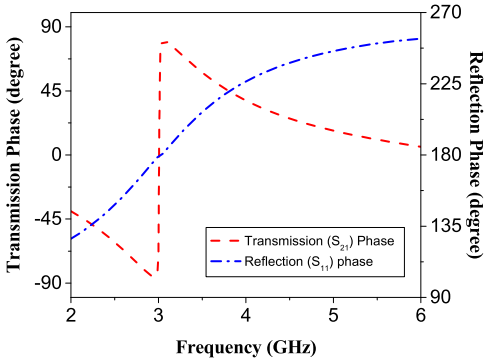

FIGURE 4. Simulated transmission and reflection phase of the planar FSS for normal incidence of plane wave.

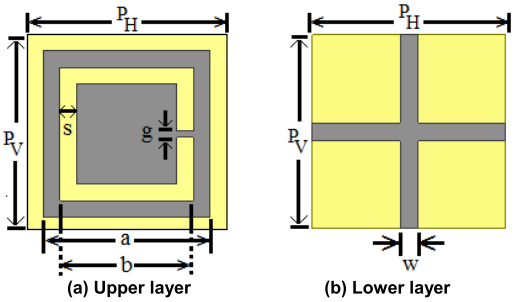

FIGURE 5. Unit cells of the dual-layer FSS-based corner reflector (All dimensions in millimeters).

shaped FSS exhibits wideband response [31] whereas loop shaped FSS exhibits compact unit cell dimension on the order of quarter wavelength and better angular stability [32]–[34]. The split ring is chosen instead of simple square loop for the purpose of fine tuning of the resonating frequency by changing the gap in the split ring. The patch area is 10.5 mm × 10.5 mm which is close to $\lambda_g/4$. The cross grid in the bottom layer is added in order to achieve a passband at 3 GHz with a phase of zero degree so that the antenna radiation at 3 GHz is not affected by the corner reflector. The reason being, the spacing between the FSS-based corner reflector and the antenna is less than half-wavelength value at 3 GHz that causes impedance mismatch of the antenna at 3 GHz whereas the flat FSS screen being at a distance larger than half-wavelength value at 5.5 GHz does

TABLE 2. Dimensions of unit cell of the dual-layer FSS (5.5 GHz).

Parameter	$P_H = P_V$	a	b	g	s	w
Value	11 mm	10.5 mm	8.6 mm	0.4 mm	1 mm	1 mm

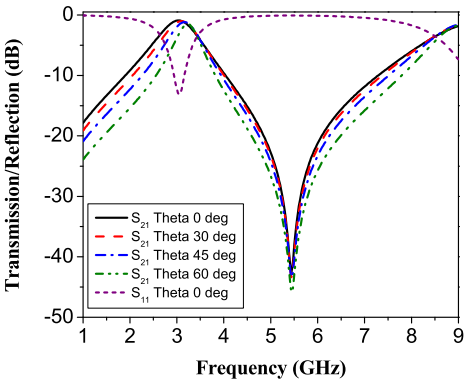

FIGURE 6. Simulated transmission coefficients (S_{21}) of the FSS for different angles (theta) of incident plane wave in the Transverse Electric plane and reflection coefficient (S_{11}).

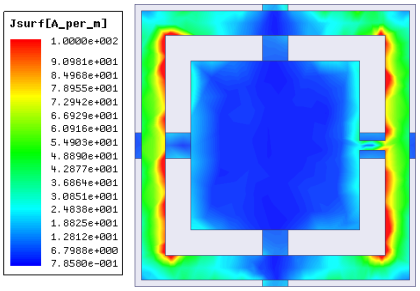

FIGURE 7. Surface current distribution (A/m) on the unit cell of the dual-layer FSS at 5.5 GHz.

not causes significant impedance mismatch at this frequency. The dimensions of the unit cells for upper and lower FSS layers for the corner reflector are listed in Table 2.

Simulated transmission and reflection coefficients of the FSS are plotted in Fig. 6 and the corresponding phase responses are plotted in Fig. 8. As evident from the plot the FSS exhibits a transmission zero at 5.5 GHz leading to reflection close to 0 dB, and a transmission pole at 3 GHz leading to transmission close to 0 dB.

The FSS exhibits transmission below −10 dB reference level in 4-8 GHz leading to a bandwidth of 73% and it provides transmission above −3 dB in 2.6-3.4 GHz with a 3 dB bandwidth of 26%. The angular stability of the FSS can be observed from Fig. 6 that plots transmission response of the dual-layer FSS for various incidence angles (theta). It is evident that the FSS exhibits adequate angular stability even above 45°. The reflection at 5.5 GHz can also be realized from the surface current distribution on the dual-layer FSS as shown in Fig. 7. The current is primarily excited surrounding the slot. The phase of the FSS to be used in corner reflector is close to zero at 3 GHz which lowers the antenna's impedance mismatch further down owing to the influence of FSS loading as evident from Fig. 8. Frequency selective reflector exhibits the property of a high impedance surface in its operating frequency band. The inductive and capacitive parts of the impedance may vary, however, smaller inductance and high capacitive reactance lead to wide bandwidth. Such reflector when placed close to the antenna element affects the impedance of the antenna element too. Such impedance loading affects the antenna impedance bandwidth near 5.5 GHz. Such effect is also observed at 3 GHz where the antenna offers adequate impedance bandwidth with the FSS screen.

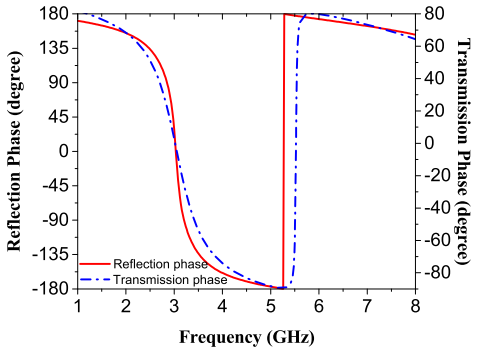

FIGURE 8. Simulated transmission and reflection phase response of the dual-layer FSS.

IV. ANTENNA WITH FSS-BASED REFLECTORS

The frequency selective corner reflector and flat reflector are placed surrounding the monopole opposite to each other above the antenna substrate as shown in the top view of the antenna in Fig. 1(a). In the present design, the use of wire monopole makes it possible to place non-planar reflectors such as corner reflector above the substrate opposite to ground plane of the antenna. With such structure, a desired beamwidth and gain of the antenna can be achieved by changing the angle between the reflecting surfaces in the corner reflector. Moreover, placing the corner reflector above the substrate opposite to antenna ground plane is easier and it helps in keeping a specific angle (here 90°) for the corner reflector in addition to offering rigidity of the design. On the other hand, such advantage cannot be achieved in case of printed antenna as it does not have a larger and rigid ground plane with substrate. The corner reflector is placed at a distance $d_c = 34$ mm from the shorter monopole (operating at 5.5 GHz) whereas the planar meander line FSS is placed at a distance $d_f = 27$ mm from the longer monopole (operating at 3 GHz). In the proposed design, the gap between monopole and corner reflector vertex is chosen to keep a half-wavelength (at 5.5 GHz) spacing between the shorter monopole (L2) and each FSS in the corner reflector. This would make the overall phase shift of the fields reflected by the two FSSs to 0° (desired for constructive interference of the fields) as each FSS adds a phase shift of 180° to the fields. Hence such design methodology is adopted for the proposed design in the present manuscript. On the other hand,

(a) Two layers of the dual-layer FSS (5×6) operating at 5.5 GHz

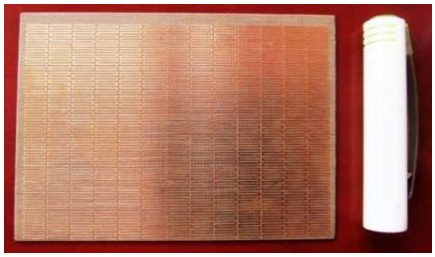

(b) The flat FSS reflector (9×15) operating at 3 GHz

(c) Antenna with the FSS layers

FIGURE 9. Fabricated prototypes of the FSS layers and Antenna and FSS.

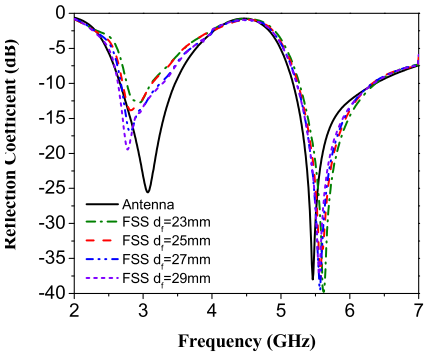

(a)

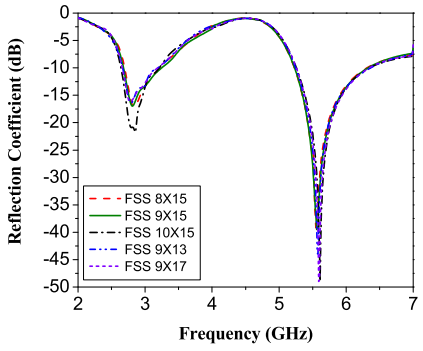

(b)

FIGURE 10. Simulated reflection coefficients (S_{11}) for the antenna with the meander line FSS only for (a) different values of spacing 'd_f' and (b) different size of the FSS array.

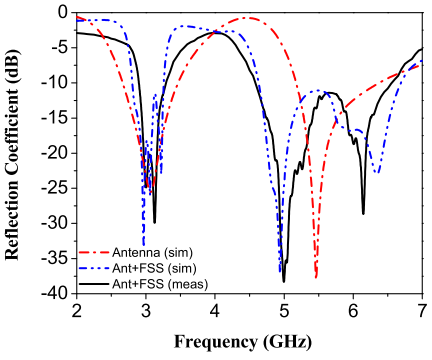

FIGURE 11. Simulated and measured reflection coefficients (S_{11}) for the antenna with both the reflectors.

the planar FSS operating at 3 GHz is placed at a spacing of λ/4 from the antenna as the surface adds a phase shift near 180° and by doing so the surface exhibits constructive interference of the signals radiated by the antenna leading to gain enhancement at 3 GHz. Thus, the two frequency selective reflectors, when used along with each other make a triangle surrounding the antenna. Moreover the gap between the two surfaces is kept owing to the individual spacing of the FSSs from the antenna under consideration as explained above. A further extension of such design by elongating the FSSs in the corner reflector to minimize the gap would lead to non-functioning of the unit cells at the edges – hence such design is also avoided.

Fabricated prototypes of the FSS screens in the flat and corner reflectors as well as that of the antenna-FSS composite structure are shown in the Fig. 9. The antenna with planar FSS in the form of meander line is simulated using ANSYS make HFSS v19.0 for studying the variation of reflection coefficient (S_{11}) with change in operating frequency. The reflection coefficients of the antenna with flat FSS only are shown in Fig. 10(a) and (b) for variation in antenna-FSS spacing and FSS array size respectively. It can be seen from Fig. 10 (a) that with the introduction of FSS the resonating frequencies are shifted due to impedance loading. The FSS reflector is a high impedance surface and thus when placed close to the antenna affects the impedance matching according to the surface reflection phase. The reflector has a reflection phase close to zero at 3 GHz. As a result the antenna impedance matching is not affected significantly by the variation in antenna-reflector spacing in the 3 GHz frequency band. The resonating frequency of the antenna in the 5.5 GHz band has a small shift with the variation in antenna-FSS spacing because of the fact that the reflector has a phase much beyond zero near 5.5 GHz that affects the impedance matching of the monopole antenna element in this band.

In order to keep the spacing close to the quarter-wavelength value at 3 GHz (i.e. 25 mm), d_f is chosen as 27 mm. The effect of variation in the FSS array size, on the antenna S_{11} is also studied and the results are shown in Fig. 10(b). The variation in array size increases the number of unit cells in the reflector. Additional unit cells get excited by the fields in the antenna radiation leading to flow of surface current on them. Such unit cells also become reflective in the operating band (here 3 GHz). However it does not change the property of the high impedance surface such as reflector phase. Thus an increase in the size of the FSS panel does not change the antenna impedance matching and reflection coefficient by a significant amount. To maintain the height of the planar FSS close to that of the corner reflector, a 9×15 array is chosen. Simulated and measured S_{11} of the antenna with both the FSS screens, are shown in Fig. 11. The antenna exhibits wide impedance bandwidth near 5.5 GHz due to the corner reflector, whereas the impedance matching is improved near 3 GHz due to the inductive grid shaped FSS layer on the back side of the corner reflector screens. In its operating band the FSS reflector exhibits a phase near 180° as evident from Fig. 8. As a result the high impedance surface exhibits a change in the impedance matching of the antenna near 5.5 GHz thereby increasing the -10 dB bandwidth of the antenna-FSS composite structure. The inductive grids exhibit a transmission pole near 3 GHz as shown in Fig. 6. With the transmission pole the FSS exhibits a phase around zero degree at 3 GHz (Fig. 8) that in turn prevents the degradation of impedance matching of the antenna at this frequency.

The antenna's radiation pattern in terms of its simulated values and measured values including and excluding FSS screens are plotted are shown in Fig. 12 for 3 GHz and in Fig. 13 for 5.5 GHz. Both co-polar and cross-polar components are plotted. For better understanding, the co-polar patterns of the antenna with only the planar FSS screen, is included in the plot.

It can be seen from Fig. 12(a) that with the introduction of the planar FSS, the antenna radiation becomes directive in the XY plane, whereas the beamwidth gets reduced from 102° to 78° with the addition of the corner reflector, as confirmed by the measurement. The corner reflector being transparent at 3 GHz, lead to constructive interference of the waves radiated towards phi = 180° (negative x direction). The radiation in the XZ plane is maximum near theta = 67°. The Front-to-Back ratio (F/B) is improved more with the corner reflector as compared to planar FSS with meander lines.

The cross-polarization level of the antenna at 3 GHz becomes more with the corner reflector due to the square grids. The possible reason is that the grids are independent of horizontal and vertical polarization and adds to the radiation in orthogonal polarization plane. The radiation plots in the Fig. 13(a) and (b) reveals that, with the flat FSS, the antenna keeps omni-directional radiation in the XY and XZ plane but with a small amount of variation (4 dB) in the XY plane, whereas the radiation becomes highly directive with the addition of corner reflector, as confirmed by the measurement. The corner reflector does not affect the cross-polarization level at 5.5 GHz, as the split ring shaped slot loaded patch in the corner reflector, is polarization dependent and its response changes in the plane of orthogonal polarization.

The variation of antenna gain with frequency in the 4.5-6.5 GHz band with and without FSS, are shown in Fig. 14. Simulation and measurement results are plotted. It can be

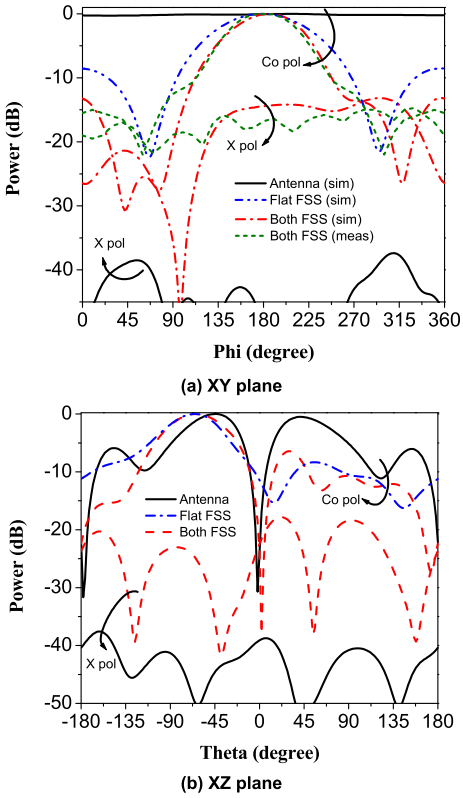

FIGURE 12. Simulated and measured radiation patterns of the antenna with and without FSS screens at 3 GHz.

TABLE 3. Characteristics of the antenna with and without FSS-based flat and corner reflectors.

Parameter	Frequency		Antenna	Flat FSS	Both FSS	
					Simulated	Measured
Bandwidth (%)	3 GHz		26%	21%	15%	12.9%
	5.5 GHz		20%	19%	42%	40%
Beamwidth (3 dB)	3 GHz	XY	360°	102°	78°	70°
		XZ	57°	62°	66°	-
	5.5 GHz	XY	360°	<360°	38°	42°
		XZ	40°	48°	36°	-
Peak gain (dBi)	3 GHz		3.8 dBi	7.6 dBi	8 dBi	7.1 dBi
	5.5 GHz		4 dBi	5.8 dBi	14 dBi	12.2 dBi
F/B ratio (XY plane)	3 GHz		0.2 dB	8.5 dB	13.2 dB	15.5 dB
	5.5 GHz		1.3 dB	4 dB	23 dB	20 dB
Radiation efficiency	3 GHz		96%	92%	84%	-
	5.5 GHz		94%	89%	86%	-

TABLE 4. Comparison of proposed antenna performance with the existing designs.

Parameters	Frequency		3 dB beamwidth		Peak gain		3 dB gain bandwidth		Dimension (mm×mm)	Design technology
Band	1st	2nd	1st	2nd	1st	2nd	1st	2nd		
Ref [16]	10.5 GHz	12.3 GHz	23°	15°	18.2 dBi	20.5 dBi	7.5%	8.7%	110×110 3.9λ×3.9λ	PRS with dipole slots above antenna
Ref [21]	2.4 GHz	2.4 GHz	45°	30°	11.0 dBi	14.0 dBi	-	-	300×212 2.4λ×1.7λ	Dipole with metallic corner reflector
Ref [18]	10.6 GHz	13.2 GHz	26°	22°	14.5 dBi	15.1 dBi	4.5%	4.6%	110×110 3.9λ×3.9λ	Dual band EBG layers on antenna
Ref [20]	800 MHz	2 GHz	88°	49°	6.8 dBi	8.9 dBi	-	-	500×500 1.3λ×1.3λ	Metal and FSS-based flat reflectors
Ref [23]	5.5 GHz	4.1 GHz	31°	17°	10.6 dBi	16.7 dBi	-	-	160×120 2.2λ×1.6λ	FSS superstrate with inductive strips
Present design	3.0 GHz	5.5 GHz	70°	42°	7.1 dBi	12.2 dBi	10%	36%	110×59 1.1λ×0.2λ	FSS-based flat and corner reflectors

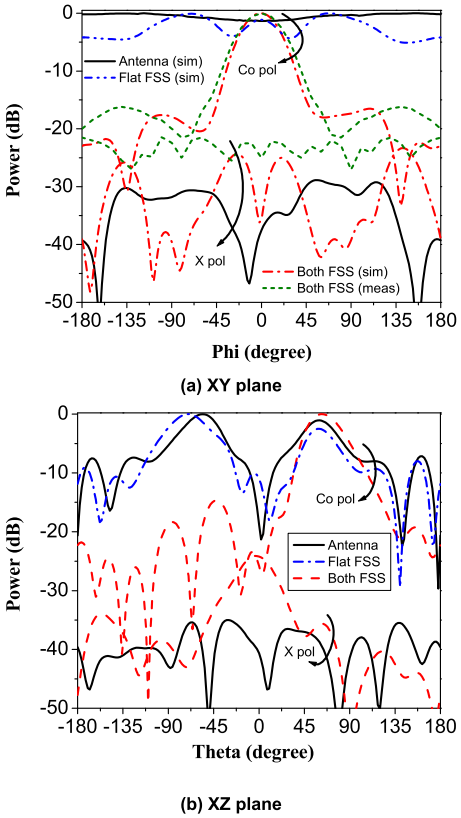

FIGURE 13. Simulated and measured radiation patterns of the antenna with and without FSS screens at 5.5 GHz.

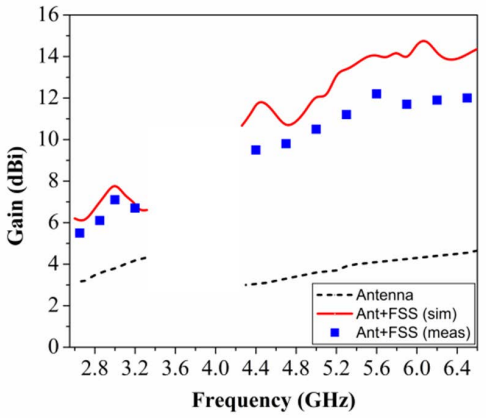

FIGURE 14. Simulated and measured gain of antenna with and without the FSS-based corner reflector (5 × 6) and the flat FSS reflector (9 × 15) for d_c = 34 mm and d_f = 27 mm.

observed that the corner reflector based on FSS in the proposed design also improves the antenna gain by 8-10 dB and the operation is unaffected by the planar FSS. Three-dimensional gain plots of the composite structure at 3 GHz and 5.5 GHz are shown in Fig. 15(a) and (b) respectively. As evident, the proposed antenna exhibits directive radiation at 3 GHz as well as at 5.5 GHz but with different beamwidth and directivity.

Simulated and measured parameters of the antenna such as impedance bandwidth (−10 dB), beamwidth (3 dB), are listed in the Table 3. In terms of beamwidth, peak gain and F/B ratio, the corner reflector exhibits more directive radiation at 5.5 GHz with higher gain compared to the radiation at 3 GHz with moderate gain due to flat shape of the FSS.

The antenna beamwidth at 3 GHz can be varied by changing the shape of the FSS reflector. Such design can be achieved by using flexible dielectric substrate of dielectric constant close to that of the substrate being used for the FSS at 3 GHz. The substrate material need to be ultra thin and polymer can be used for this purpose. The FSS reflector designed on such flexible substrate may be bent with a specific curvature. Variation in beamwidth of the antenna-reflector structure may be achieved by varying radius of curvature of the surface. Variation in beamwidth of antenna radiation at 5.5 GHz can be obtained by changing the angle of the corner reflector that in turn changes the number of images. This leads to variation of field strength of the antenna in the far field resulting in beamwidth variation.

Table 4 enlists a comparative study of the parametric values of the proposed antenna along with other similar structures available in literature. The proposed design achieves directive radiation in both the bands, with different beamwidths. The difference in gain of the proposed design and the others is due to the difference in beamwidths. The present design achieves more beamwidth in the first and second band with suitable

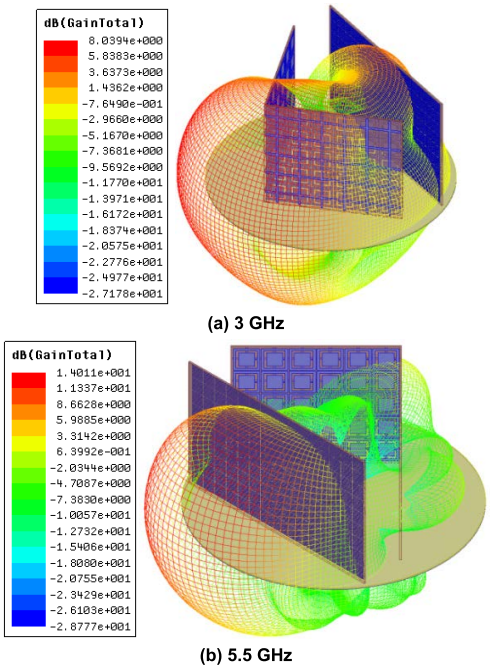

FIGURE 15. Simulated three-dimensional radiation plots of the antenna with the FSS-based flat (9 × 15) and corner reflectors (5 × 6) for $d_c = 34$ mm and $d_f = 27$ mm.

gains, compared to others except [22]. The proposed antenna with the FSS-based flat and corner reflectors, exhibits more 3 dB gain bandwidth in both the bands, compared to all other works in the Table. In terms of dimension the design is low profile compared to others.

V. CONCLUSION

The use of frequency selective corner reflector and flat reflector for achieving diverse beam radiation in a dual-band monopole antenna is studied in the present design. Unlike the FSS amalgamated in the corner reflector exhibiting reflective response at 5.5 GHz and transmissive response at 3 GHz, the same used in case of flat reflector exhibits opposite response. Accordingly the antenna exhibits directive radiation at both the frequencies, however in two opposite directions. Unit cell of the FSS at 3 GHz is of the order of $\lambda_g/11$, leading to low-profile design. The antenna exhibits both wide beamwidth at 3 GHz and narrow beamwidth at 5.5 GHz with high gain in the range of about 8-14 dBi by using different orientations of the reflectors. The proposed antenna is basically a prototype which can be further deployed for satellite communication, Ground Penetrating Radar (GPR), and other applications if made of suitable materials like Al-Mg-Alloy, carbon fiber reinforced plastic material or Invar/Titanium/fiber glass-epoxy. Moreover the proposed antenna can be enclosed in a hypothetical cube of dimension 110 × 110 × 59 mm^3 ($1.1\lambda \times 1.1\lambda \times 0.2\lambda$) thereby reflecting compatibility to be fitted in a small space. Thus the antenna can be used in applications such as satellite communication, GPR etc. owing to its physical viability and mechanical stability.

REFERENCES

[1] H. Ullah and F. A. Tahir, "A high gain and wideband narrow-beam antenna for 5G millimeter-wave applications," *IEEE Access*, vol. 8, pp. 29430–29434, 2020.
[2] M. Stanley, Y. Huang, H. Wang, H. Zhou, A. Alieldin, and S. Joseph, "A capacitive coupled patch antenna array with high gain and wide coverage for 5G smartphone applications," *IEEE Access*, vol. 6, pp. 41942–41954, 2018.
[3] M. Moosazadeh, "High-gain antipodal vivaldi antenna surrounded by dielectric for wideband applications," *IEEE Trans. Antennas Propag.*, vol. 66, no. 8, pp. 4349–4352, Aug. 2018.
[4] S. M. Sifat, M. M. M. Ali, S. I. Shams, and A.-R. Sebak, "High gain bow-tie slot antenna array loaded with grooves based on printed ridge gap waveguide technology," *IEEE Access*, vol. 7, pp. 36177–36185, 2019.
[5] Z. Zaharis, E. Vafiadis, and J. N. Sahalos, "On the design of a dual-band base station wire antenna," *IEEE Antennas Propag. Mag.*, vol. 42, no. 6, pp. 144–151, Dec. 2000.
[6] S.-H. Chen, J.-S. Row, and K.-L. Wong, "Reconfigurable square-ring patch antenna with pattern diversity," *IEEE Trans. Antennas Propag.*, vol. 55, no. 2, pp. 472–475, Feb. 2007.
[7] W. K. Toh, Z. N. Chen, X. Qing, and T. S. P. See, "A planar UWB diversity antenna," *IEEE Trans. Antennas Propag.*, vol. 57, no. 11, pp. 3467–3473, Nov. 2009.
[8] X. Wang, Z. Feng, and K. M. Luk, "Pattern and polarization diversity antenna with high isolation for portable wireless devices," *IEEE Antennas Wireless Propag. Lett.*, vol. 8, pp. 209–211, 2009.
[9] A. Ourir, K. Rachedi, D.-T. Phan-Huy, C. Leray, and J. de Rosny, "Compact reconfigurable antenna with radiation pattern diversity for spatial modulation," in *Proc. 11th Eur. Conf. Antennas Propag. (EUCAP)*, Paris, France, Mar. 2017, pp. 3038–3043.
[10] M. Gallo, E. Antonino-Daviu, M. Ferrando-Bataller, M. Bozzetti, J. M. Molina-Garcia-Pardo, and L. Juan-Llacer, "A broadband pattern diversity annular slot antenna," *IEEE Trans. Antennas Propag.*, vol. 60, no. 3, pp. 1596–1600, Mar. 2012.
[11] S. X. Ta, I. Park, and R. W. Ziolkowski, "Dual-band wide-beam crossed asymmetric dipole antenna for GPS applications," *Electron. Lett.*, vol. 48, no. 25, pp. 1580–1581, Dec. 2012.
[12] J. Ouyang, F. Yang, S. Yang, and Z. Nie, "A novel E-shape radiation pattern reconfigurable microstrip antenna for broadband, wide-beam, high-gain applications," *Microw. Opt. Technol. Lett.*, vol. 50, no. 8, pp. 2052–2054, 2008.
[13] Y. Q. Zhang, S. T. Qin, X. Li, and L. X. Guo, "Novel wide-beam cross-dipole CP antenna for GNSS applications," *Int. J. RF Microw. Comput.-Aided Eng.*, vol. 28, no. 6, 2018, Art. no. e21272.
[14] A. C. Balanis, *Antenna Theory: Analysis and Design*, 3rd ed. Hoboken, NJ, USA: Wiley, 2005.
[15] L. Sun, W. Huang, B. Sun, Q. Sun, and J. Fan, "Two-port pattern diversity antenna for 3G and 4G MIMO indoor applications," *IEEE Antennas Wireless Propag. Lett.*, vol. 13, pp. 1573–1576, 2014.
[16] Y. Ge and K. P. Esselle, "A method to design dual-band, high-directivity EBG resonator antennas using single-resonant, single-layer partially reflective surfaces," *Prog. Electromagn. Res. C*, vol. 13, pp. 245–257, 2010.
[17] L. Leger, R. Granger, M. Thevenot, T. Monediere, and B. Jecko, "Multi-frequency dielectric EBG antenna," *Microw. Opt. Technol. Letters*, vol. 40, no. 5, pp. 420–423, Mar. 2004.
[18] B. A. Zeb, Y. Ge, K. P. Esselle, Z. Sun, and M. E. Tobar, "A simple dual-band electromagnetic band gap resonator antenna based on inverted reflection phase gradient," *IEEE Trans. Antennas Propag.*, vol. 60, no. 10, pp. 4522–4529, Oct. 2012.
[19] C. Biancotto and P. Record, "Dielectric EBG corner reflector antenna," *J. Electromagn. Waves Appl.*, vol. 24, nos. 14–15, pp. 2107–2118, Jan. 2010.
[20] H. So, A. Ando, T. Seki, M. Kawashima, and T. Sugiyama, "Directional multi-band antenna employing frequency selective surfaces," *Electron. Lett.*, vol. 49, no. 4, pp. 243–245, Feb. 2013.
[21] T. D. Dimousios, S. A. Mitilineos, S. C. Panagiotou, and C. N. Capsalis, "Design of a corner-reflector reactively controlled antenna for maximum directivity and multiple beam forming at 2.4 GHz," *IEEE Trans. Antennas Propag.*, vol. 59, no. 4, pp. 1132–1139, Apr. 2011.
[22] A. Edalati and T. A. Denidni, "High-gain reconfigurable sectoral antenna using an active cylindrical FSS structure," *IEEE Trans. Antennas Propag.*, vol. 59, no. 7, pp. 2464–2472, Jul. 2011.

[23] M. Wang, C. Huang, P. Chen, Y. Wang, Z. Zhao, and X. Luo, "Controlling beamwidth of antenna using frequency selective surface superstrate," *IEEE Antennas Wireless Propag. Lett.*, vol. 14, pp. 1014–1017, 2015.
[24] K. Krishnamoorthy, B. Majumder, J. Mukherjee, and K. P. Ray, "Low profile pattern diversity antenna using quarter-mode substrate integrated waveguide," *Prog. Electromagn. Res. Lett.*, vol. 55, pp. 105–111, 2015.
[25] Y. Zheng, G. A. E. Vandenbosch, and S. Yan, "Low-profile broadband antenna with pattern diversity," *IEEE Antennas Wireless Propag. Lett.*, vol. 19, no. 7, pp. 1231–1235, Jul. 2020.
[26] X. Liu, Y. Wu, Z. Zhuang, W. Wang, and Y. Liu, "A dual-band patch antenna for pattern diversity application," *IEEE Access*, vol. 6, pp. 51986–51993, 2018.
[27] F. Huang, J. C. Batchelor, and E. A. Parker, "Interwoven convoluted element frequency selective surfaces with wide bandwidths," *Electron. Lett.*, vol. 42, no. 14, pp. 788–790, Jul. 2006.
[28] M. B. Yan, S. Qu, J. Wang, J. Zhang, and A. Zhang, "A novel miniaturized frequency selective surface with stable resonance," *IEEE Antennas Wireless Propag. Lett.*, vol. 13, pp. 639–641, 2014.
[29] S. N. Azemi, K. Ghorbani, and W. S. T. Rowe, "Angularly stable frequency selective surface with miniaturized unit cell," *IEEE Microw. Wireless Compon. Lett.*, vol. 25, no. 7, pp. 454–456, Jul. 2015.
[30] A. B. Varuna, S. Ghosh, and K. V. Srivastava, "A miniaturized-element bandpass frequency selective surface using meander line geometry," *Microw. Opt. Technol. Lett.*, vol. 59, no. 10, pp. 2484–2489, 2017.
[31] A. B. Munk, *Frequency Selective Surfaces: Theory and Design*, 1st ed. New York, NY, USA: Wiley, 2000.
[32] A. Kapoor, R. Mishra, and P. Kumar, "Frequency selective surfaces as spatial filters: Fundamentals, analysis and applications," *Alexandria Eng. J.*, vol. 61, no. 6, pp. 4263–4293, Jun. 2022.
[33] A. Egemen and M. Kuzuoglu, "Design of the square loop frequency selective surfaces with particle swarm optimization via the equivalent circuit model," *Radioengineering*, vol. 18, no. 12, pp. 95–102, Jun. 2009.
[34] S. M. Mahmood and T. A. Denidni, "Switchable square loop frequency selective surface," *Prog. Electromagn. Res. Lett.*, vol. 57, pp. 61–64, 2015.
[35] A. Chatterjee and S. K. Parui, "Performance enhancement of a dual-band monopole antenna by using a frequency-selective surface-based corner reflector," *IEEE Trans. Antennas Propag.*, vol. 64, no. 6, pp. 2165–2171, Jun. 2016.
[36] A. Chatterjee and S. K. Parui, "Frequency-dependent directive radiation of monopole-dielectric resonator antenna using a conformal frequency selective surface," *IEEE Trans. Antennas Propag.*, vol. 65, no. 5, pp. 2233–2239, May 2017.

AYAN CHATTERJEE (Member, IEEE) was born in West Bengal, India, in 1988. He received the M.Tech. degree in communication engineering from the University of Kalyani, in 2012, and the Ph.D. degree in microwave engineering from the Indian Institute of Engineering Science and Technology (IIEST), Shibpur, in 2018.

From 2012 to 2013, he served as an Assistant Professor with the Department of Electronics and Communication Engineering (ECE), SKFGI, West Bengal. From 2018 to 2021, he worked as an Assistant Professor with the Department of ECE, National Institute of Technology, Sikkim. He is currently an Associate Professor with the Department of ECE, University of Engineering and Management Kolkata. He is the author of more than 50 papers in referred journals and conference proceedings. His research interests include frequency selective surfaces, artificial magnetic conductors, slot antennas, and ultra-wideband antennas.

Dr. Chatterjee is a Senior Member of URSI. He received a Senior Research Fellowship from the Council of Scientific and Industrial Research, Government of India, in 2014. He is a Reviewer of several international journals, such as IEEE Access, IEEE Transactions on Antennas and Propagation, IEEE Antennas and Wireless Propagation Letters, IEEE Transactions on Microwave Theory and Techniques, *Microwave and Optical Technology Letters*, and *Journal of Electromagnetic Waves and Applications*.

SOUMEN BANERJEE (Senior Member, IEEE) received the B.Sc. degree (Hons.) in physics from the University of Calcutta, in 1998, the B.Tech. and M.Tech. degrees in radio physics and electronics from the Institute of Radio Physics and Electronics, University of Calcutta, in 2001 and 2003, respectively, and the Ph.D. degree in engineering from the Indian Institute of Engineering Science and Technology (IIEST), Shibpur, India.

He was a Visiting Faculty with the Department of Applied Physics, University of Calcutta. He is currently the Head of the Department of Electronics and Communication Engineering, University of Engineering and Management, Kolkata, India. He has a teaching/research experience of more than 20 years. He has published more than 100 contributory papers in journals and international conferences. He has authored ten books and five book chapters in fields of communication engineering, electromagnetic field theory, microwave, and antenna. He has edited three books published by Springer. His profile is included in IBC, Cambridge, England; and Marquis Who's Who in the World, USA. His current research interests include design, fabrication and characterization of wide band gap semiconductor-based IMPATT diodes at D band, W-band and THz frequencies, SIW technology-based antennas, printed antennas and arrays, FSS, dielectric resonator antennas, body wearable antennas, machine learning, fuzzy systems, and evolutionary computation.

Dr. Banerjee is a Senior Member of IEEE (USA) and IEEE AP Society. He is also a fellow of IETE, New Delhi, India. He is a Reviewer of several international journals, such as IEEE Transactions on Emerging Topics in Computational Intelligence, IEEE Transactions on Electron Devices, IEEE Access, IEEE Sensors Letters, *Microwave and Optical Technology Letters* (MOTL-Wiley), *Journal of Electromagnetic Waves and Applications* (Taylor and Francis), *Radioengineering Journal* (Czech and Slovak Technical University), *Journal of Computational Electronics* (Springer-Nature), *Journal of Renewable and Sustainable Energy* (American Institute of Physics-AIP), *Cluster Computing* (Springer-Nature), and *Journal of Infrared, Millimeter and Terahertz Waves* (Springer-Nature). He acted as a Convener in international conferences, like OPTRONIX-2019 (IEEE) and OPTRONIX-2020 (Springer) both held at Kolkata, India, and also chaired many technical sessions in several international conferences.

JAROSLAV FRNDA (Senior Member, IEEE) was born in Martin, Slovakia, in 1989. He received the M.Sc. and Ph.D. degrees from the Department of Telecommunications, VSB—Technical University of Ostrava, in 2013 and 2018, respectively.

He has been working as an Assistant Professor with the Department of Quantitative Methods and Economic Informatics under the Faculty of Operation and Economics of Transport and Communicationsat, University of Žilina, Slovakia, since 2019. He has authored and coauthored 18 SCI-E and nine ESCI articles in WoS. His research interests include quality of multimedia services in IP networks, data analysis, and machine learning algorithms.

MAREK DVORSKY was born in Czech Republic, in 1981. He received the master's degree from the VSB—Technical University of Ostrava, FEECS, in 2004.

Since 2006, he has been working as a Research Fellow with the VSB—Technical University of Ostrava. In 2009, he successfully defended his dissertation thesis. He is working as an Assistant Professor with the Department of Telecommunications. His most of the activities cover antenna engineering and radio-wave propagation. He has authored dozens of scientific and technical publications. Since 2008, he has been interested in magnetic loop antennas (MLA). He published about MLA five successful monographies. His recent concern is around the Internet of Things. His research interest includes digital radio communication technologies.